doi.org/10.36721/PJPS.2025.38.5.REG.14207.1

Hepatoprotective effects of albiziasaponin-A, ellagitannin and azadirachtin in iron-intoxicated animal model

Tahira Anwar[1], Sikandar Hayat[1], Iftikhar Ali[2], Arif Malik[1,3] and Malik Ihsan Ullah Khan[1]*

[1]Institute of Molecular Biology and Biotechnology, The University of Lahore, Pakistan
[2]Department of Life Sciences, School of Science, The University of Management and Technology (UMT), Lahore, Pakistan
[3]School of Pain and Regenerative Medicine, The University of Lahore, Pakistan

Abstract: Prolonged exposure to iron can result in severe hepatic complications such as chronic liver damage, jaundice, cirrhosis, and hepatocellular carcinoma. Current treatment options for metal-induced hepatotoxicity are limited and often associated with undesirable side effects. This study investigates the hepatoprotective and anti-inflammatory properties of three phytochemicals, albiziasaponin-A, ellagitannin and azadirachtin, against iron-induced liver toxicity. Both *in silico* and *in vivo* approaches were employed to assess their binding affinity as well as the therapeutic effects of selected phytochemicals against the target protein, cyclooxygenase-2, a marker of liver damage. Molecular docking revealed strong binding affinities of all compounds with COX-2, indicating promising anti-inflammatory potential. Hepatic injury was assessed through biomarkers including ALT, 4HNE, 8-OHdG, TNF-α, IsoP-2α, MDA, and COX-2 levels. The rat group exposed to iron overdose exhibited significantly elevated biomarker levels compared to controls, confirming hepatotoxicity. However, combination therapy with the selected phytochemicals led to a significant reduction in these biomarkers, suggesting effective hepatoprotection. These findings indicate that albiziasaponin-A, ellagitannin and azadirachtin possess potent therapeutic properties that may be beneficial in mitigating iron-induced liver damage. Further investigation is needed to establish their potential for inclusion in novel drug formulations targeting inflammatory liver diseases.

Keywords: *In silico studies*, azadirachtin, albiziasaponin-A, ellagitannin, COX-2 inhibitor, anti-inflammatory.

Submitted on 03-03-2025 – Revised on 16-04-2025– Accepted on 28-05-2025

INTRODUCTION

Iron is a vital element for all living organisms, contributing to numerous essential metabolic processes such as DNA synthesis, mitochondrial function, energy production, blood formation (hematopoiesis), and oxygen transport (Crichton *et al*., 2002). Iron deficiency leads to anemia, while excessive iron accumulation can also result in hemochromatosis. In excess, iron facilitates Fenton reactions, leading to the generation of harmful reactive oxygen species (ROS) (Crichton *et al*., 2002; Galaris *et al*., 2008). The liver is especially vulnerable to ROS-induced damage, and iron storage can worsen conditions like chronic hepatitis and cirrhosis (Lin *et al*., 2008). The safe amount of iron that is non-toxic for the biological system is around 20 mg/kg body weight. (Thorngren *et al*., 2016). Increased iron level, such as 20-60mg/kg body weight, can induce adverse medical conditions including heart attack, osteoarthritis, diabetes mellitus, metabolic syndrome, osteoporosis, hypothyroidism, and sometimes even leads to death (Bassett *et al*., 2011). Clinical iron toxicity progresses through five stages, but not all patients do not experience each stage due to the concentration of iron deposition. Common symptoms in the first stage include vomiting, abdominal pain, diarrhoea and hematemesis. The second stage, the deceptive recovery phase, can occur even with high iron levels. Shock, metabolic acidosis and renal failure characterize in the third stage. Hepatic failure and elevated aminotransferase levels occur in the fourth stage and the fifth and final stage involves the restoration of gastrointestinal mucosa (Dardashti *et al*., 2024).

Macromolecules such as proteins, lipids and carbohydrates are susceptible to oxidative damage. Increased iron levels lead to the induction of lipid peroxidation, resulting in increased levels of ROS and oxidative stress (Imam *et al*., 2017). Hydrogen peroxide (H_2O_2) and superoxide (O_2) are considered toxic radicals that are responsible for increased lipid peroxidation, resulting in the formation of by-products such as, 4-Hydroxynonenal and 4-Hydroxy-2, 3-alkenals. These act as active mediators in several signaling cascades and play significant role in the proliferation of target cells. (Krylatov *et al*., 2018). Increased production of ROS induces oxidative stress, which exacerbates damage at the cellular or molecular level. Hemochromatosis is a genetic condition characterized by the abnormal accumulation of iron within the body, hereditary hemochromatosis (HFE) or non-HFE mutations are considered as genetic defects. Exposure to excess environmental iron leads to severe hepatotoxicity and induces pro-fibrogenic cofactors resulting from viral hepatitis, hepatotoxic xenobiotics or chronic alcohol abuse (Licata *et al*., 2021).

**Corresponding author:* e-mail: ihsan.ullah@lmbb.uol.edu.pk

Albizia procera, known as white siris, belongs to the Fabaceae family. It is mainly found in India, Myanmar and Southeast Asia. One of its major phytocompounds, albiziasaponin-A, play a significant hepatoprotective role. Its roots are a source of the natural herbicide mesotrione (Srivastava *et al*., 2020). *Azadirachta indica*, commonly known as neem, belongs to the Meliaceae family and is found in the Indian subcontinent. Azadirachtin, a compound in neem, is effective in treating hepatic damage induced by carbon tetrachloride (CCl_4) and has various medicinal uses, including anti-inflammatory and hypoglycemic properties. Albiziasaponin-A is effective in modulating immune responses and reducing inflammation by inhibiting pro-inflammatory mediators and enzymes (Fernandes and Tambourgi, 2023). Studies have shown that albiziasaponin-A can downregulate the expression of inflammatory cytokines and enzymes involved in the inflammatory response, such as cyclooxygenase-2 (COX-2) (Wang *et al*., 2020). Similarly, ellagitannin, polyphenolic compounds found in various fruits and nuts such as pomegranates and walnuts, have been selected for their potent anti-inflammatory and antioxidant effects. Ellagitannins scavenge free radicals and inhibit inflammatory pathways, including the activity of COX-2, which is critical for the synthesis of pro-inflammatory prostaglandins, thereby reducing inflammation and associated symptoms (Gandhi *et al*., 2024).

Presently, computational approaches such as molecular docking are being used to assess the binding behaviour of chemical compounds to target proteins. Previous research has generated widespread interest in various phytoconstituents (i.e., alkaloids, terpenoids and phenolics) demonstrating their efficacy against inflammatory disorders (Bellik *et al*., 2012a, Bellik *et al*., 2012b). Based on a comprehensive literature survey three phytocompounds (Albiziasaponin-A, Ellagitannin and Azadirachtin) were selected to evaluate their docking interactions with COX-2, a key mediator of inflammatory pathways and an inducible early response gene activated in response to various extracellular or intracellular physiological stimuli (Gandhi *et al*., 2017). Additionally, *in vivo* experiments were performed to evaluate the therapeutic effects of these phytochemicals against hepatotoxicity in albino wistar rats.

MATERIALS AND METHODS

Computational methodology

The canonical amino acid sequence (Accession No. P35355; 604 AA) of COX-2 from Rat (*Rattus norvegicus*) was retrieved from Uniprot Knowledgebase Database (https://www.uniprot.org/) in FASTA format. Position-Specific Iterative Basic Local Alignment Search Tool (Psi. BLAST) (Samal *et al*., 2021) was used to obtain a suitable template for protein model generation (Li *et al*., 2011). The best template was selected based on sequence identity and query coverage. Modeller v9.17 was employed to generate three-dimensional (3D) structure (Chandrasekaran *et al*., 2017). Couple of commands align2d.py and get-model.py were employed in cmd to obtain the best protein model. Furthermore, different evaluation tools ERRAT, Verify3D and Rampage were used to evaluate of predicted model structure. The overall quality factor of generated 3D model was identified from ERRAT (Chowdhury *et al*., Samant *et al*., 2015) whereas, the allocation of favoured, allowed and outliers regions of model protein were confirmed through Rampage (Chandrasekaran *et al*., 2017). Finally, USCF Chimera v1.12 was used to minimize the model protein structure at 1000 steepest and 1000 conjugate gradient runs with Amber force field parameters (Medoro *et al*., 2024).

Designing of ligands and molecular docking

Active phytocompounds, including albiziasaponin-A (21604181), Ellagitannin (10033935), and Azadirachtin (5281303) were confirmed and sourced from ChemSpider and PubChem (Jha *et al*., 2022). The compounds were converted into three-dimensional Mol2 format using Open Babel (Bhat *et al*., 2022). The accuracy of these homology models was assessed through four validation tests: Procheck, ERRAT, Z-score, and VERIFY 3D. These evaluations confirmed the models' reliability and appropriateness for molecular docking studies (Reyes-Gastellou *et al*., 2021). Homology models for COX-2 were constructed with Swiss Model, using murine COX-2 crystal structures as templates. Molecular docking was initiated by analyzing the COX-2 binding sites in detail. Ligand-binding residues were precisely identified by superimposing structures co-crystallized with inhibitors (Kiss *et al*., 2012).

The pharmacokinetic properties like Absorption, Distribution, Metabolism, Excretion, and Toxicity (ADMET) profile were calculated from the admetSAR online server (Cheng *et al*., 2012). Before, the docking binding pocket was identified through literature (Orlando *et al*., 2015) and CASTP (Zhang *et al*., 2011), COACH (Yang *et al*., 2013), and 3D-Ligandsite (Wass *et al*., 2010) tools. A molecular docking study was performed through AutoDock Vina using the standard protocol. The grid values were adjusted as X=156, Y=150, and Z=65 against the target protein before the final run of the docking experiment. The docked complexes were evaluated based on energy values (Kcal/mol) and binding interaction behaviour. The graphical depiction was generated by UCSF Chimera v1.12 and Discovery Studio, respectively.

Plants extract

The standardized extract of albiziasaponin-A, ellagitannin, and azadirachtin was purchased from the Sigma Aldrich Corporation (St. Louis, MO, USA), and different doses of the extract were prepared according to the study design.

Study design and experimental analysis

The experiment was performed at the animal house of the Institute of Molecular Biology and Biotechnology (IMBB) of the University of Lahore. This experimental work was performed according to the departmental ethical research committee guidelines (IRB: SPRM/UOL/MOCT/D01/0116).

The animals were randomly divided into nine groups; each group had five Wister Albino Rats. Group A was the control healthy rats with no toxicity. Hepatotoxicity induced through the iron @150mg/kg b.wt/d (90 days) in Group B served as disease positive. Group C, D, E was induced hepatotoxicity through iron and treated with the single therapy of Albiziasaponin-A, Ellagitannin, Azadirachtin @400mg/kg b. wt. respectively. The animals were treated with iron and fed with a combination of two plants (Albiziasaponin-A + Ellagitannin) in group F. Group G was treated with iron and administered the mixture of two plants (Albiziasaponin-A + Azadirachtin). Combination therapy of two plants (Ellagitannin + Azadirachtin) was given to the iron-treated rats in Group H. Rats were fed with the mixture of three plants (Albiziasaponin-A + Ellagitannin + Azadirachtin), which had iron-induced liver toxicity in Group I, as shown in Table 4. The data were subjected to analyses of variance using a COSTAT computer package (CoStat software, Berkley, California). The mean values were compared with the least significant difference test following Snedecor and Cochran. Statistical analysis was performed using one-way analysis of variance (ANOVA) followed by Duncan S' Multiple Range test (DMR-Test). The values are Mean±SD, and p values ($p<0.05$) were considered significant.

Biochemical analysis

Levels of 3,4-Methylenedioxyamphetamine (MDA) were measured through thiobarbituric acid reactive substances (TBARs) by following previously provided protocols (Papastergiadis *et al*., 2012). Whereas levels of Alanine transaminase (ALT), tumor Necrosis Factor alpha (TNF-α), 8-hydroxy-2'-deoxyguanosine (8-OHdG), 4HNE, and Isoprostanes isoprostane-2 alpha (ISOP-2α) were measured through a commercially available enzyme-linked immunosorbent assay (ELISA) Kit.

Measurement of MDA levels

Levels of MDA were quantified using the TBARs assay. The protocol followed was provided by previously provided (Ganhão *et al*., 2011). Briefly, samples were mixed with TBA reagent and incubated at high temperatures (typically around 95°C) for a specific period (60 minutes). After cooling, the absorbance of the pink chromogen was measured at 532 nm, providing an estimate of the MDA concentration in the sample.

Measurement of ALT, TNF-α, 8OHdG, 4HNE, and isoprostanes

The levels of ALT, TNF-α, 8OHdG, 4HNE, and isoprostanes were determined using commercially available ELISA kits, which are widely recognized for their sensitivity and specificity. The general steps followed in the ELISA protocol for each biomarker were:

Sample preparation

Blood was collected, and serum was separated and diluted as required by the kit protocols.

Antigen-antibody reaction

Prepared samples were added to wells coated with specific antibodies for each target biomarker. The samples were incubated to allow binding between the antigen (biomarker) and the immobilized antibody.

Washing

Unbound substances were removed by washing the wells multiple times with a wash buffer.

Detection antibody

A biotinylated detection antibody specific to the target biomarker was added to the wells, followed by incubation.

Streptavidin-HRP conjugate

Streptavidin conjugated to horseradish peroxidase (HRP) was added, which binds to the biotinylated detection antibody.

Substrate addition

A substrate solution, typically containing tetramethylbenzidine (TMB), was added to the wells. The HRP enzyme catalyzes a colorimetric reaction, producing a blue color that changes to yellow upon addition of the stop solution.

Measurement

The absorbance of the yellow color was measured at a wavelength of 450 nm using a microplate reader. The absorbance values were directly proportional to the concentration of the target biomarker in the samples.

RESULTS

Protein model analysis

The generated protein model was analysed through computational tools. The evaluation tool indicated that the protein model demonstrated good accuracy and residues were plumpted in a favourable region. ERRAT analysis of the statistics of non-bonded interactions between different atom types yielded a score that justifies the accuracy of the model protein. Our results showed that the COX-2 model protein exhibited a good an ERRAT value of 93.34%. Additionally, the verify 3D (90.04%) score also confirmed the accuracy of the target protein. Ramachandran analysis

showed that most residues were present in the favoured region (87.6%), with a single outlier observed in the Ramachandran graph. The predicted model of COX-2 is shown in fig. 1.

Fig. 1: Generated model of COX-2.

Phytochemical analysis

Pharmacokinetic analysis of phytochemicals

The three selected phytochemicals are shown in fig. 2. These phytochemicals were subjected to AdmetSAR to predict their ADMET properties. Among the three compounds, Albiziasaponin-A exhibited positive behaviour in crossing the blood brain barrier (BBB), whereas the other two, Ellagitannin and Azadirachtin showed negative behvior for the BBB parameter. For human intestinal absorption, all three demonstrated positive behavior and have potential to be absorbed in the intestine. Additionally, low CYP inhibitory potential was observed for all three compounds. Albiziasaponin-A showed a value of 0.9360, as compared to other two compounds (Ellagitannin and Azadirachtin values) 0.7364 and 0.8863, respectively. Non-AMES toxicity and non-carcinogens behavior were observed for all three compounds. The overall results indicate that Albiziasaponin-A exhibited good therapeutic behavior compared to the other two compounds (table 1).

Molecular docking analysis

Binding energy of phytochemicals

All three phytochemicals bound to the target protein at the active site and exhibited favorable binding affinity values (Kcal/mol). Table 2 depicts the binding energies, with Albiziasaponin-A exhibiting a high binding energy value (-15.0 Kcal/mol) compare to the other compounds. Ellagitannin showed a comparable enrgy value to Albiziasaponin-A, whereas, Azadirachtin had a binding energy of -11.3 Kcal/mol.

Binding interactions

The docking complexes were analyzed based on hydrogen and hydrophobic interactions. In the interaction between In Albiziasaponin A-COX-2 docking complex, interactions occurred via GLN356, GLN355, PHE353 and HIS108 hydrogen bonds. The ellagitannin-COX-2 complex interacted via hydrogen bonds with LYS82, PRO177, GLN178, ASN567, SER565 whereas the Azadirachtin-COX-2 complex showed hydrogen bonds interaction at ASN19 and PRO140. The 3D structures of all three docking complexes are shown in fig. 3 (A, B, C). Comparative analysis revealed that common residues were observed in all docking complexes, with different bonds detailed in table 3.

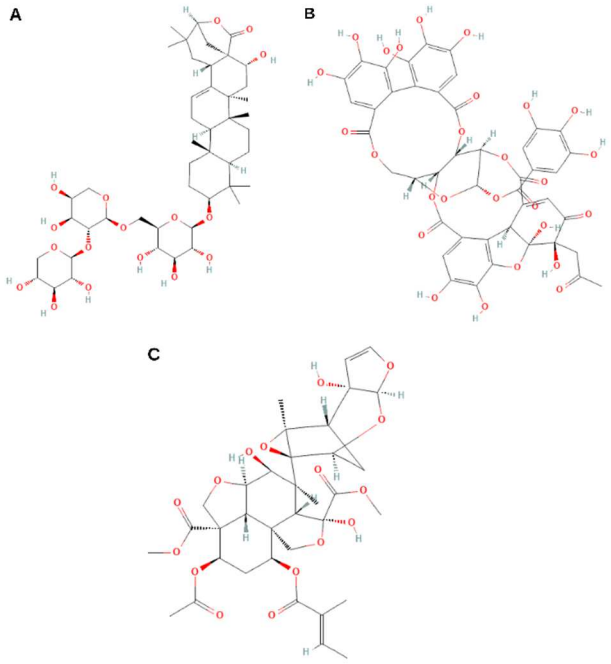

Fig. 2: Phytochemical structures of Albiziasaponin-A, Ellagitannin, and Azadirachtin, sourced from PubChem, with identifier numbers 21604181, 10033935 and 5281303, respectively.

In vivo analysis

Quantification of serum level of ALT

Experimental design groups used in current studies are presented in table 4. The results shown in table 5 revealed that the level of ALT was 37.129±1.99 IU/L (p=0.0012) in the control group of rats. When rats were exposed to iron, the levels of ALT increased to 116.96±7.86 IU/L in this group, in contrast to the healthy group. Iron-treated rats orally administered albiziasaponin-A (400 mg/kg b. Wt) exhibited a significant reduction in ALT levels (81.10±9.06 IU/L). Iron-induced rats administered a singular treatment of Ellagitannin also showed decreased levels of ALT to 60.16±5.06 IU/L, which is lower than that observed with albiziasaponin-A. When the iron-treated rat group was orally administered with Azadirachtin, the level of ALT was reduced to 50.26±2.66 IU/L. The combination therapy (in groups F, G, and H) of two compounds more effectively decreased the ALT level than the single treatment group.

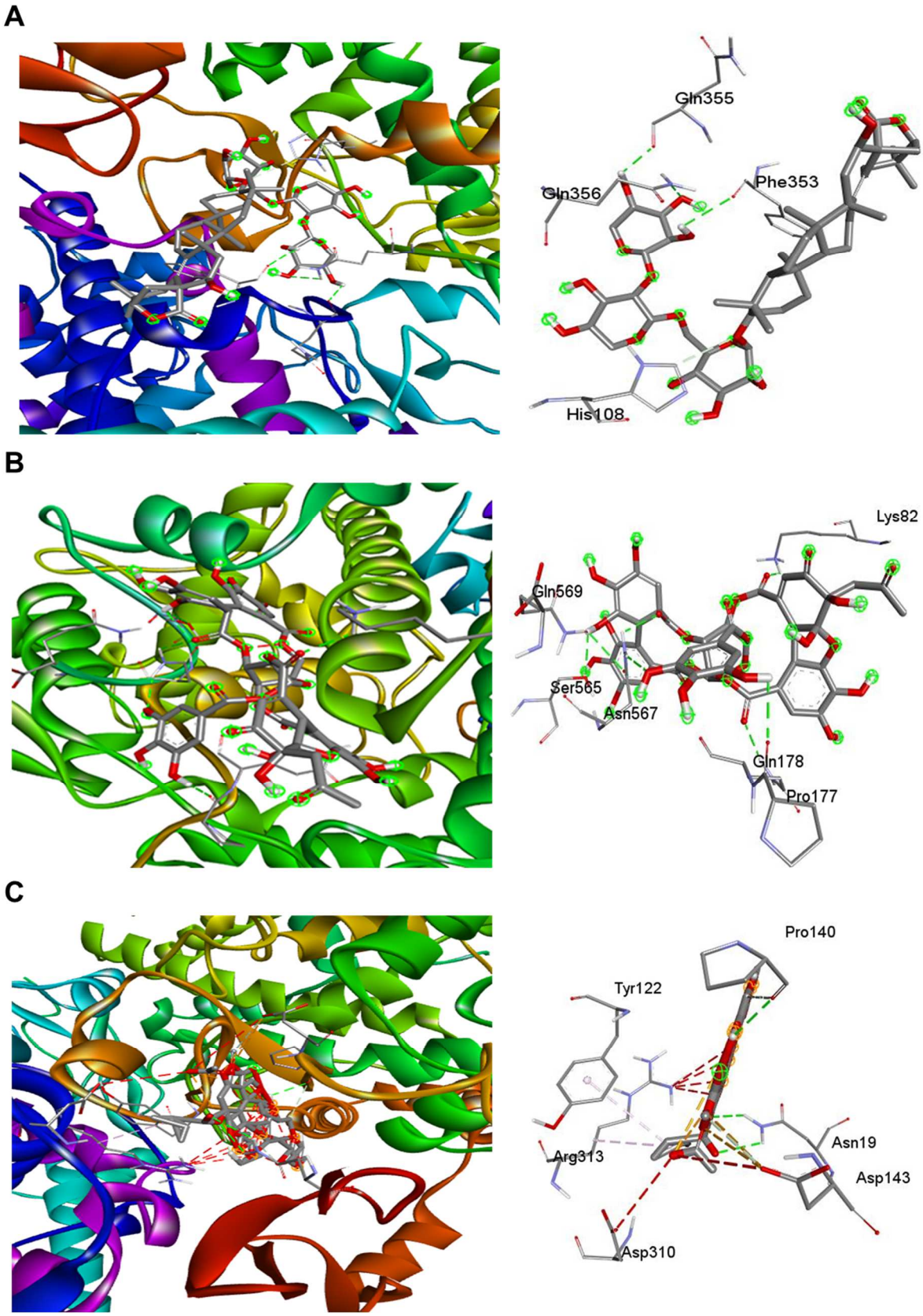

Fig. 3: The docking complexes of all three phytocompounds; Albiziasaponin-A (A), Ellagitannin (B) and Azadirachtin (C) with COX-2.

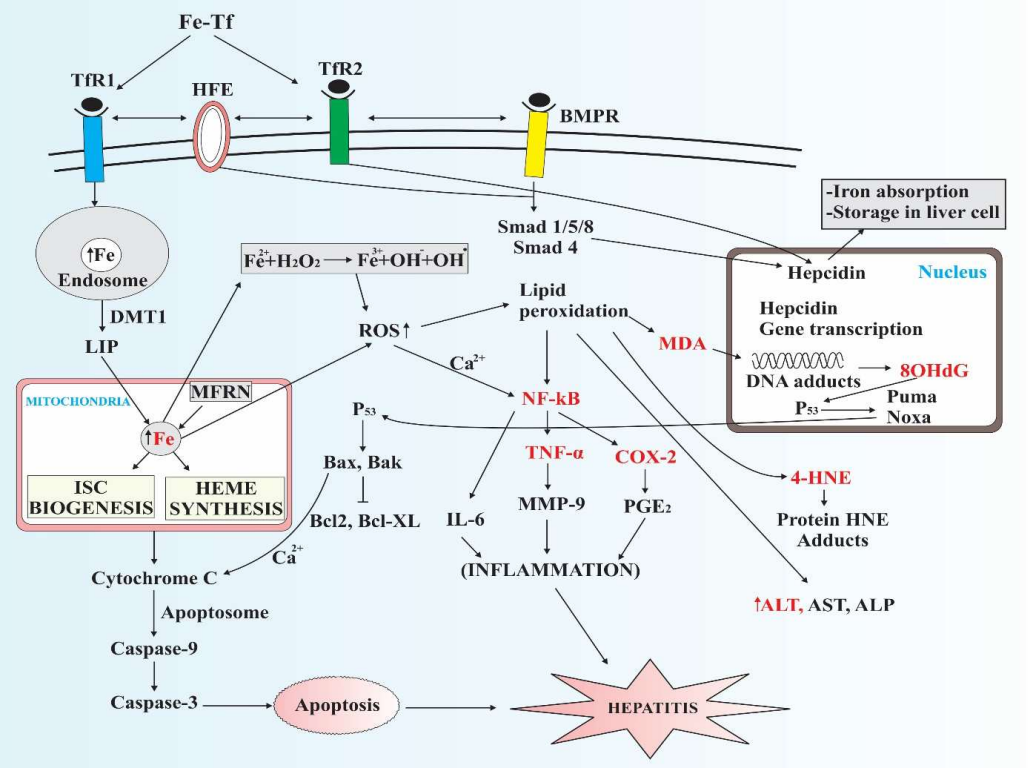

Fig. 4: Iron binds with transferrin protein (Tf) that is involve for the transportation of iron from blood to cellular system through specific type of receptor that is exist in divalent form and depend on HFE protein. The activation of the BMP signaling pathway leads to nuclear translocation of SMAD1/5/8 with SMAD4 and activate the hepcidin transcription. Through interactions between transferrin receptor 1 (TfR1), HFE and transferrin receptor 2 (TfR2) hepcidin levels are controlled in response to extracellular iron status. After the induction of iron into the cytosol it might be enter into the endosome and disassociate from its binding protein. Additionally, iron further becomes a part of labile iron pool (LIP) with the help of DMT1. In this response iron enter into the mitochondria either by Ca symptom channels or directly enter through LIP and cause the oxidative stress through the overloading of iron NADPH oxidase. In the mitochondrial membrane mitoferrin (MFRN) isoforms are involve through the direct communication of endosome with mitochondria and from LIP to mitochondrion direct iron uptake It is well known that during the oxidative stress the free radicals were binds with membrane and initiate the lipid peroxidation that's results in the level of oxidative biomarkers include MDA, 8OHdG, 4HNE were increases. ROS directly regulate the inflammatory biomarker including NFkB. NFkB activate IL-6, TNF-α and Cox-2. TNF-α activate MMP-9 and Cox-2 activate PG E_2 then MMP-9 and PG E_2 involve in inflammation and regulate in steatohepatitis. Furthermore 8-OHdG activate the P_{53} in nucleus. P_{53} activates Puma and Noxa. Puma and Noxa activate P_{53} in cytosol then these apoptotic proteins Bax and Bak activate then these activated proteins activate P_{53} in mitochondria. Cytochrome C releases then apoptosis occur through caspase-9 and caspase-3.

Table 1: ADMET properties of selected phytocompounds.

Properties	Albiziasaponin-A	Ellagitannin	Azadirachtin
Blood Brain Barrier	BBB+, 0.5000	BBB-, 0.6212	BBB-, 0.7733
Human Intestinal Absorption	HIA+, 0.6748	HIA+, 0.8930	HIA+, 0.8895
CYP Inhibitory	Low, 0.9360	Low, 0.7364	Low, 0.8863
AMES Toxicity	Non-AMES Toxic 0.8943	Non-AMES Toxic 0.6290	Non-AMES Toxic 0.7563
Carcinogens	Non-Carcinogens 0.9692	Non-Carcinogens 0.9680	Non-Carcinogens 0.9455
Acute Oral Toxicity	III 0.5590	III 0.4614	I 0.6952
Biodegradation	Not ready biodegradable 0.9868	Not ready biodegradable 0.8477	Not ready biodegradable 1.000
Aqueous Solubility (Logs)	-4.2181	-3.1958	-3.8348

Table 2: Binding affinities of selected phytocompounds with COX-2.

Docked complexes	Binding affinities (Kcal/mol)
Albiziasaponin-A with COX-2	-15.0 Kcal/mol
Ellagitannin with COX-2	-14.3 Kcal/mol
Azadirachtin with COX-2	-11.3 Kcal/mol

The synergistic effect of all three phytocompounds on the rat group demonstrated a significant decrease in ALT level to 20.663±3.28 IU/L, within the normal range. The maximum reduction in ALT level was observed only in the last combination group.

4-HNE quantification

The normal 4-HNE level was 2.27±3.096 ng/L (p= 0.0156), measured in the control group, and after iron accumulation, the 4-HNE level increased to 16.36±1.29 ng/L, as shown in table 5. Treatment with Albiziasaponin-A reduced the 4-HNE level to 13.09±2.02 ng/L. Individual treatment of Ellagitannin and Azadirachtin reduced 4-HNE levels to 10.09±2.09 ng/L and 43.49±3.45 ng/L, respectively. The combination of three therapies decreased 4-HNE levels more effectively than individual therapy, as shown in table 5. The maximum decrease in 4-HNE levels (5.06±1.08 ng/L) was observed with the combination of all three compounds, compared to the control group levels.

8-OHDG quantification

Oral iron administration (150mg/kg b. Wt) increased 8-OHdG levels in rats to 61.19±2.59 pg/ml, compared to the normal group (4.29±0.26 pg/ml, p=0.0125) as presented in table 5. Individual treatment with Albiziasaponin-A, Ellagitannin, and Azadirachtin (400mg/kg b. Wt) in iron-induced rats significantly decreased 8-OHdG levels to 20.09±3.08 pg/ml, 25.20±4.09 pg/ml, and 17.39±3.28 pg/ml, respectively, compared to untreated groups. The combination of Albiziasaponin-A and Ellagitannin, Albiziasaponin-A and Azadirachtin, and Ellagitannin and Azadirachtin significantly decreased 8-OHdG levels to 9.09±2.08 pg/ml, 10.06±1.20 pg/ml, and 9.09±4.06 pg/ml, respectively, compared to individual treatment. Maximum normalization of 8-OHdG level (7.09±1.99 pg/ml) was observed in the combination of all three compounds.

Determination of TNF-α level

The normal level of TNF-α in the control group was 19.59±2.28 ng/ml shown in table 5. When healthy rats were treated with iron then the level of TNF-α (72.24±4.48 ng/ml) significantly increased, in contrast to the healthy rats. The level of TNFα was reduced to 55.19±1.56 ng/ml, 57.33±5.59 ng/ml, and 35.26±3.76 ng/ml after individual treatment with Albiziasaponin-A, Ellagitannin, and Azadirachtin, respectively. The value of TNF-α (85.06±5.06 ng/ml) increased significantly when the mixture of Albiziasaponin-A and Ellagitannin was administered, and the combination of Albiziasaponin-A and Azadirachtin and Ellagitannin and Azadirachtin significantly reduced the level of TNF-α to 25.10±6.09 ng/ml and 29.06±4.20 ng/ml, respectively. When all phytochemicals (Albiziasaponin-A, Ellagitannin, and Azadirachtin) were administered, the maximum decrease in the level of TNF-α (18.06±3.26 ng/ml) was observed.

Determination of isoP-2α level

Table 5 showed that in the control group, IsoP-2α level was 23.45±1.39 pg/ml (p=0.000), and iron induction raised the IsoP-2α level to 151.96±6.16 pg/ml. Albiziasaponin-A in iron-treated rats reduced IsoP-2α to 112.28±9.98 pg/ml. Ellagitannin decreased IsoP-2α significantly to 88.06±5.55 pg/ml compared to other groups, and Azadirachtin did not significantly decrease IsoP-2α (88.86±9.66 pg/ml). The combination of Albiziasaponin-A and Ellagitannin resulted in 77.36±4.20 pg/ml IsoP-2α, Albiziasaponin-A and Azadirachtin reduced IsoP-2α to 78.96±9.40 pg/ml, and Ellagitannin and Azadirachtin decreased IsoP-2α to 65.09±7.33 pg/ml compared to individual treatment groups. The combination of Albiziasaponin-A, Ellagitannin, and Azadirachtin effectively normalized the IsoP-2α level to 30.06±4.277 pg/ml across all groups.

Determination of MDA level

According to table 5, when the healthy rats were treated with the iron metal than the level of MDA (7.98±2.16 nmol/ml) was increased in contrast to the control group (1.19±0.066 nmol/ml). When iron-induced rat groups were individually treated with Albiziasaponin-A, Ellagitannin, and Azadirachtin, they showed a notable reduction in the MDA level to 3.19±1.17 nmol/ml, 6.79±2.79 nmol/ml and 5.65±3.98 nmol/ml respectively. Iron-intoxicated rats treated with the combination of two phytochemicals Albiziasaponin-A and Ellagitannin, Albiziasaponin-A and Azadirachtin, and Ellagitannin and Azadirachtin, the level of MDA was significantly reduced, as shown in table 5. A highly effective and significant change in MDA levels was observed with the combination of Albiziasaponin-A, Ellagitannin, and Azadirachtin, with a remarkable decrease in MDA levels to 2.19±31.987 nmol/ml, and the results were statistically significant, with Pearson's' correlation coefficients presented in table 6.

Determination COX-2 level

Cyclooxygenase-2 is an enzyme that produces prostaglandins and is highly inducible, particularly in inflammatory conditions. In healthy rats, Cox-2 level was 0.51±0.042 ng/ml (p=0.017), and iron increased COX-2 to 4.09±3.67 ng/ml as shown in table 5. Higher COX-2 level observed in Albiziasaponin-A treated group while Ellagitannin and Azadirachtin reduced COX-2 to 2.69±1.29 ng/ml, 0.09±0.960 ng/ml respectively.

Table 3: Interactive residues of COX-2 utilizing AutoDock Vina.

COMPOUNDS	TYPE OF BONDING	AMINO ACID RESIDUES
Ellagitannin	Conventional Hydrogen Bond	LYS82, PRO177, GLN178, ASN567, SER565
	Unfavorable Donor	GLN569
Albiziasaponin A	Conventional Hydrogen Bond	GLN356, GLN355, PHE353
	Carbon Hydrogen Bond	HIS108
Azadirachtin A	Conventional Hydrogen Bond	ASN19, PRO140
	Carbon Hydrogen Bond	PRO140
	Pi-Alkyl	TYR122
	Alkyl	ARG313
	Attractive Charge	ASP143

Table 4. Experimental design.

GROUPS (n=5)	TREATMENTS
A	Control
B	Fe alone
C	Fe + Albiziasaponin-A
D	Fe + Ellagitannin
E	Fe + Azadirachtin
F	Fe + Albiziasaponin-A+Ellagitannin
G	Fe + Albiziasaponin-A+Azadirachtin
H	Fe + Ellagitannin +Azadirachtin
I	Fe + Albiziasaponin-A+Ellagitannin Azadirachtin

Dose of Fe (150mg /kg B.Wt. per week)
Dose of Albiziasaponin-A, Ellagitannin, Azadirachtin (400 mg/kg B.Wt.)

Table 5. Biochemical response of Albiziasaponin-a, Ellagitannin, and Azadirachtin in a rat model.

GROUPS	MEAN±SD (n=10)						
	ALT (IU/L)	4-HNE (ng/L)	8-OHdG (pg/ml)	TNF-α (ng/ml)	IsoP-2α (pg/ml)	MDA (nmol/ml)	COX-2 (ng/ml)
A	37.129±1.99	2.27±3.096	4.29±0.26	19.59±2.28	23.45±1.39	1.19±0.066	0.51±0.042
B	116.96±7.86	16.36±1.29	61.19±2.59	72.24±4.48	151.96±6.16	7.98±2.16	4.09±3.67
C	81.10±9.06	13.09±2.02	20.09±3.08	55.19±1.56	112.28±9.98	3.19±1.17	4.18±2.90
D	60.16±5.06	10.09±2.09	25.20±4.09	57.33±5.59	88.06±5.55	6.79±2.79	2.69±1.29
E	50.26±2.66	43.49±3.45	17.39±3.28	35.26±3.76	88.86±9.66	5.65±3.98	0.09±0.960
F	47.86±9.10	15.06±5.06	9.09±2.08	85.06±5.06	77.36±4.20	5.09±3.88	3.08±0.99
G	40.66±5.29	19.06±5.06	10.06±1.20	25.10±6.09	78.96±9.40	4.99±2.67	1.89±3.098
H	39.76±4.19	8.18±1.91	9.09±4.06	29.06±4.20	65.09±7.33	8.89±1.90	0.89±0.155
I	20.663±3.28	5.06±1.08	7.09±1.99	18.06±3.26	30.06±4.277	2.19±1.987	2.36±1.857
LSD (0.05)	4.66	7.95	6.56	10.26	8.16	1.22	1.33
p-VALUE	0.0012	0.0156	0.0125	0.0113	0.000	0.0081	0.017

Table 6: Pearson s' correlation coeeficients of different variables in liver tissues of rats receiving iron.

VARIABLES	ALT	AFP	8-OHdG	TNF-α	IsoP-2α	MDA	COX-2
ALT	1	0.733**	0.461**	0.663**	0.715**	0.662**	0.704*
4-HNE		1	0.617*	0.680**	0.6 19**	0.460**	0.416**
8-OhdG			1	0.564**	0.504**	0.645**	0.509**
TNF-α				1	0.692**	0.594**	0.629**
IsoP-2α					1	0.516**	0.658**
MDA						1	0.711**

** Correlation is significant at the 0.01 level (two-tailed).

The combination of Albiziasaponin-A and Azadirachtin and Ellagitannin and Azadirachtin treatments significantly decreased COX-2 to 1.89±3.098 ng/ml and 0.89±0.155 ng/ml respectively. The combination of all three phytochemicals in iron-induced rats showed a significant reduction in COX-2 (2.36±1.857 ng/ml), approaching the normal level, as presented in table 5. COX-2, as an inflammatory marker, showed a significant correlation with other biomarkers, as indicated in table 6.

DISCUSSION

The domain of drug design and development has witnessed substantial advancements in recent years, marked by the emergence of innovative computational methodologies that enhance the discovery and optimization of novel therapeutic agents (Kumar *et al*., 2011). In silico approaches have facilitated the identification and development of herbal medicinal agents with reduced toxicity profiles compared to conventional therapeutic interventions (Taylor *et al*., 2001). The current investigation was structured to systematically characterize the therapeutic potential of diverse phytochemical constituents against iron induce hepatotoxicity through integrated *in silico* and *in vivo* experimental frameworks. The phyto medicines play a crucial role in the field of novel drug designing (Thomford *et al*., 2018). The plants derived phytocompounds have considerable focus as anti-inflammation agents and prevention from the inflammation process (Shin *et al*., 2020). Molecular docking analyses were performed using plant-derived phytocompounds Albiziasaponin-A, Ellagitannin, and Azadirachtin (fig. 2) against COX-2 (fig. 1) to evaluate the efficacy of the utlized phytocompounds against inflammation. All three selected phytocompounds showed effective anti-inflammatory activity against the COX-2. In the development of new drug, *in silico* ADMET and molecular docking studies are commonly utilized due to cost effective and reduced time consumption compared to lab experiments (Bandaru *et al*., 2021). All three phytocompounds exhibited favorable ADMET properties as anti-inflammatory agents (table 1). A good drug molecule should reach the target site at a sufficient dose and remain bioactive to achieve the anticipated biological activity, thereby meeting the medication outcome (Daina *et al*., 2017). The ADMET properties of phytocompounds were satisfactory, as they are non-carcinogenic, exhibit low CYP inhibitory potential, and all compounds demonstrate the ability to be absorbed. The molecular properties of small compounds, including bioavailability and membrane permeability, are always dependent on LogP. Molecular docking was conducted to gain an understanding with structural specificities, conformational behavior, and stability of ligand target complexes (Pandey *et al*., 2017; Shukla *et al*., 2018). It provides an atomic-level characterization of the molecular process and stability analysis of protein ligand complexes (Hassan *et al*., 2020). Table 2 showed that higher binding affinity of Albiziasaponin-A with COX-2 (-15.0 Kcal/mol), followed by two other phytocompounds (Ellagitannin (-14.3 Kcal/mol) and Azadirachtin (-11.3 Kcal/mol) as compared to the standard drug diclofenac (-7.3 kcal/mol) (Uzzaman *et al*., 2021). All three phytocompounds demonstrated the highest binding affinity with lowest energy; however, Albiziasaponin-A showed better potential of inhibition as well as binding affinity as an anti-inflammatory agent. The binding strength and catalytic activity between COX-2 and phytocompounds are predicted as hydrogen bonds, along with carbon bonds, Pi-Alkyl, and opposite charge attraction, as well (table 3). Albiziasaponin-A-COX-2 docking complex interacts via hydrogen bonds with GLN356, GLN355, PHE353, and HIS108. The Ellagitannin-COX-2 interacts via hydrogen bonds with LYS82, PRO177, GLN178, ASN567, SER565, whereas Azadirachtin-COX-2 exhibits hydrogen bond interactions at ASN19 and PRO140 as shown in fig. 3. These residues may inhibit the inflammation process of COX-2, as they have been previously reported as active sites of COX-2 (Kiefer *et al*., 2000).

Iron overload disrupts cellular metabolism, leading to severe diseases by impairing mitochondrial function. Mitoferrin isoforms, involved in the direct communication between endosomes and mitochondria, facilitate iron uptake from the labile iron pool to the mitochondrion (Rouault, 2012), with the proposed mechanism presented in fig. 4. Azadirachtin, a limonoid derivative of *Azadirachta indica*, has been extensively studied for its hepatoprotective properties. An analysis by Baligar *et al*. (2014) demonstrated that azadirachtin-A exhibits significant protective effects against carbon tetrachloride (CCl4)-induced hepatotoxicity in Wistar rats, normalizing liver enzymes and improving histopathology. Ellagitannins are utilized for hepatotoxicity, liver fibrosis, and hepatocellular carcinoma in various parts of the world. When oxidative stress produced in the cell, it acts against them by producing antioxidants (Teodor *et al*., 2020). The combination of the three phytochemicals significantly decreased ALT, oxidative stress markers (4-HNE, 8-OHdG, MDA), and proinflammatory cytokines (TNF-α, COX-2, IsoP-2) in the animal model, as shown in table 5. These findings underscore the synergistic effects of the three drugs, which exceed the efficacy observed with individual or double combinations. Overproduction of ROS disrupts normal cellular activity and leads to lipid peroxidation. Lipid peroxidation produced 4-hydroxynonenal and malondialdehyde (Ayala, Munoz, & Argüelles, 2014). 4-HNE exhibits a positive correlation with 8-HdG (0.617*), TNF-α (0.680**), IsoP-2α (0.619**), MDA (0.460**) and COX-2 (0.416**) as shown in table 6. MDA, an end product of lipid peroxidation, plays a vital role in damaging DNA by forming DNA adducts in the nucleus (Ayala, Munoz, & Argüelles, 2014). MDA shows a positive correlation with

COX-2 (0.711**). 8-OHdG, a byproduct of DNA oxidation by ROS, accelerates recovery from inflammation when treated (Ye *et al*., 2023). Furthermore, according to the results of the current study, 8-OHdG exhibits a positive correlation with MDA (0.645**) and TNF-α (0.564**) as a liver damage factor. 8-OHdG contributes to inflammation and shows a positive correlation with IsoP-2α (0.504**) and COX-2 (0.509**). TNF-α is a cytokine and cell signalling protein involved in inflammation, inhibits the production of cytokines, affects cell survival and regulates DNA transcription while activating IL-6, TNF-α, and Cox-2 (Tajdari *et al*., 2024). Inflammation mediated by TNF-α can lead to increased oxidative stress, resulting in the production of IsoP-2. Our study observed similar findings, with TNF-α showing positive correlation with IsoP-2 (0.692**), MDA (0.594**), and COX-2 (0.629**). Increasing evidence supports the multi-component herbal therapy as a promising approach to hepatic protection. Future studies should prioritize elucidating the molecular mechanisms and exploring the potential for clinical translation.

CONCLUSION

The study findings suggest that Albiziasaponin-A, Ellagitannin, and Azadirachtin may be promising in mitigating the harmful effects of iron toxicity on liver tissues. Moreover, Albiziasaponin-A, Ellagitannin, and Azadirachtin demonstrated strong binding affinity to COX-2, as confirmed by *in silico* and *in vivo* studies. These results revealed their dual role as COX-2 inhibitors and hepatoprotective agents, as validated by biochemical analyses. Further exploration of these compounds could unveil their therapeutic and diagnostic potential, positioning them as promising candidates for anti-inflammatory interventions.

ACKNOWLEDGEMENTS

The authors would like to express their sincere gratitude to the Institute of Molecular Biology and Biotechnology (IMBB), The University of Lahore-Pakistan for providing the institutional support throughout the current analysis. We allow the participation of Waqas Safir, Computational Drug Discovery Lab (Xinjiang Key Laboratory of Biological Resources and Genetic Engineering, College of Life Sciences and Technology, Xinjiang University, Urumqi, Xinjiang, China) for its assistance in the execution of *in silico* simulations and ADMET Profiling.

Conflict of interest

Authors declare no conflict of interest.

REFERENCES

Ayala A, Muñoz MF and Arguelles S (2014). Lipid peroxidation: Production, metabolism and signaling mechanisms of malondialdehyde and 4-hydroxy-2-nonenal. *Oxid. Med. Cell Longev.*, 2014(1): 360438.

Baligar NS, Aladakatti RH, Ahmed M and Hiremath MB (2014). Hepatoprotective activity of the neem-based constituent azadirachtin-A in carbon tetrachloride intoxicated Wistar rats. *J. Physiol. Pharmacol.*, **92**(4): 267-277.

Bandaru N, Prasanth DSNBK, Reddy AR, Rao GK, Nemmani KV and Rao AN (2021). In-silico molecular docking studies of some isolated phytochemicals from *Biophytum veldkampii* against cyclooxygenase-II enzyme and *in vivo* anti-inflammatory Activity. *Pharmacogn. Res.*, **13**(4): 192-198.

Bassett ML, Hickman PE and Dahlstrom JE (2011). The changing role of liver biopsy in diagnosis and management of haemochromatosis. *Patholo.,* **43**: 433-439.

Bellik Y, Boukraa L, Alzahrani HA, Bakhotmah BA, Abdellah F, Hammoudi SM and Iguer-Ouada M (2012a). Molecular mechanism underlying anti-inflammatory and anti-allergic activities of phytochemicals: An update. *Mol.,* **18**: 322-353.

Bellik Y, M Hammoudi S, Abdellah F, Iguer-Ouada M and Boukraâ L (2012b). Phytochemicals to prevent inflammation and allergy. *Recent Pat. Inflamm. Allergy Drug Discov.,* **6**: 147-158.

Bhat BA, Mir WR, Sheikh BA, Alkanani M and Mir MA (2022). Metabolite fingerprinting of phytoconstituents from *Fritillaria cirrhosa* D. Don and molecular docking analysis of bioactive peonidin with microbial drug target proteins. *Sci. Rep.,* **12**: 7296.

Chandrasekaran G, Hwang EC, Kang TW, Kwon DD, Park K, Lee JJ and Lakshmanan VK (2017). Computational Modeling of complete HOXB13 protein for predicting the functional effect of SNPs and the associated role in hereditary prostate cancer. *Sci. Rep.,* **7**: 43830.

Cheng F, Li W, Zhou Y, Shen J, Wu Z, Liu G, Lee PW and Tang Y (2012). admetSAR: A comprehensive source and free tool for assessment of chemical ADMET properties. *J. Chem. Inf. Model.,* **52**(1): 3099-3105.

Chowdhury MHU, Das T and Sikandar S (2023). In-silico structural insights of Dengue 4 NS3 protease: Homology modeling and structural validation. *J. Phytomol. Pharmacol.,* **2**(1): 12-20.

Crichton RR, Wilmet S, Legssyer R and Ward RJ (2002). Molecular and cellular mechanisms of iron homeostasis and toxicity in mammalian cells. *J. Inorg. Biochem.*, **91**(1): 9-18.

Daina A, Michielin O and Zoete V (2017). SwissADME: A free web tool to evaluate pharmacokinetics, drug-likeness and medicinal chemistry friendliness of small molecules. *Sci. Rep.,* **7**: 42717.

Dardashti SK, Shirkhoda M, Sharifi A and Jalaeefar A (2024). Ten-year experience of reconstructive techniques after resection of hypopharyngeal squamous cell carcinoma (SCC): Changing trend from gastric pull up to free flaps. *Int. J. Cancer Manag.,* **17**: 145836.

Galaris D and Pantopoulos K (2008). Oxidative stress and iron homeostasis: Mechanistic and health aspects. *Crit. Rev. Clin. Lab. Sci.,* **45**(1): 1-23.

Gandhi GR, Antony PJ, Ceasar SA, Vasconcelos ABS, Montalvão MM, Farias De Franca MN, Resende ADS., Sharanya CS, Liu Y and Hariharan G (2024). Health functions and related molecular mechanisms of ellagitannin-derived urolithins. *Crit. Rev. Food Sci.,* **64**: 280-310.

Gandhi J, Khera L, Gaur N, Paul C and Kaul R (2017). Role of modulator of inflammation cyclooxygenase-2 in gammaherpesvirus mediated tumorigenesis. *Front. microbiol.*, **8**: 538.

Hassan SSU, Zhang WD, Jin HZ, Basha SH and Priya SS (2022). In-silico anti-inflammatory potential of guaiane dimers from *Xylopia vielana* targeting COX-2. *J. Biomol. Struct. Dyn.*, **40**(1): 484-498.

Imam MU, Zhang S, Ma J, Wang H and Wang F (2017). Antioxidants mediate both iron homeostasis and oxidative stress. *Nutri.,* **9**: 671.

Jha V, Devkar S, Gharat K, Kasbe S, Matharoo DK, Pendse S, Bhosale A and Bhargava A (2022). Screening of phytochemicals as potential inhibitors of breast cancer using structure based multitargeted molecular docking analysis. *Phytomed. plus,* **2**: 100227.

Kiefer JR, Pawlitz JL, Moreland KT, Stegeman RA, Hood WF, Gierse JK and Kurumbail RG (2000). Structural insights into the stereochemistry of the cyclooxygenase reaction. *Nat.*, **405**(6782): 97-101.

Kiss R, Sandor M and Szalai FA (2012). http://Mcule. com: A public web service for drug discovery. *J. Cheminform.,* **4**: P17.

Krylatov AV, Maslov LN, Voronkov NS, Boshchenko AA, Popov SV, Gomez L, Wang H, Jaggi AS and Downey JM (2018). Reactive oxygen species as intracellular signaling molecules in the cardiovascular system. *Curr. Cardiol. Rev.,* **14**: 290-300.

Kumar P, Pillay V, Choonara YE, Modi G, Naidoo D and Du'toit LC (2011). In silico theoretical molecular modeling for Alzheimer's disease: The nicotine-curcumin paradigm in neuroprotection and neurotherapy. *Int. J. Mol. Sci.,* **12**: 694-724.

Li J, Abel R, Zhu K, Cao Y, Zhao S and Friesner RA (2011). The VSGB 2.0 model: A next generation energy model for high resolution protein structure modeling. *Proteins:Struct., Funct., Bioinf.,* **79**: 2794-2812.

Licata A, Zerbo M, Como S, Cammilleri M, Soresi M, Montalto G and Giannitrapani L (2021). The role of vitamin deficiency in liver disease: To supplement or not supplement? *Nutri,* **13**: 4014.

Medoro A, Scapagnini G, Brogi S, Jafar TH, Trung TT, Saso L and Davinelli S (2024). Carotenoid interactions with PCSK9: Exploring novel cholesterol-lowering strategies. *J. Pharm.,* **17**: 1597.

Orlando BJ, Lucido MJ and Malkowski MG (2015). The structure of ibuprofen bound to cyclooxygenase-2. *J. Struct. Biol.,* **189**: 62-66.

Pandey T, Shukla R, Shukla H, Sonkar A, Tripathi T, and Singh AK (2017). A combined biochemical and computational studies of the rho-class glutathione s-transferase sll1545 of Synechocystis PCC 6803. *Int. J. Biol. Macromol.*, **94**: 378-385.

Reyes-Gastellou A, Jiménez-Alberto A, Castelán-Vega JA, Aparicio-Ozores G and Ribas-Aparicio RM (2021). Chikungunya nsP4 homology modeling reveals a common motif with Zika and Dengue RNA polymerases as a potential therapeutic target. *J. Mol. Model.,* **27**: 247.

Rouault TA (2012). Biogenesis of iron-sulfur clusters in mammalian cells: New insights and relevance to human disease. *Dis. Models Mech.,* **5**: 155-164.

Samal KC, Sahoo JP, Behera L and Dash T (2021). Understanding the BLAST (Basic local alignment search tool) Program and a step-by-step guide for its use in life science research. *Bhart. Kri. Anusand. Pat.,* **36**(1): 55-61.

Samant LR, Sangar VC, Khanzode M and Chowdhary A (2015). 3D modeling and characterization of HDAC9. *Ile (I),* **40**: 4.0.

Shin SA, Joo BJ, Lee JS, Ryu G, Han M, Kim WY, Park HH, Lee JH and Lee CS (2020). Phytochemicals as anti-inflammatory agents in animal models of prevalent inflammatory diseases. *Mol.,* **25**: 5932.

Shukla R, Shukla H, Sonkar A, Pandey T and Tripathi T (2018). Structure-based screening and molecular dynamics simulations offer novel natural compounds as potential inhibitors of *Mycobacterium tuberculosis* isocitrate lyase. *J. Biomol. Struct. Dyn.*, **36**(8): 2045-2057.

Srivastava V, Verma SK, Panwar S, Deep P and Verma S (2020). A brief review on phytopharmacological reports on Albizia procera. *Asian J. Pharm. Sci,* **6**: 144-149.

Tajdari M, Peyrovinasab A, Bayanati M, Rabbani MIM, Abdolghaffari AH and Zarghi A (2024). Dual COX-2/TNF-α inhibitors as promising anti-inflammatory and cancer chemopreventive agents: A review. *Iran. J. Pharm. Sci.,* **23**(1): e151312.

Taylor JLS, Rabe T, Mcgaw LJ, Jäger AK, Van Staden J (2001). Towards the scientific validation of traditional medicinal plants. *Plant Growth Regul*., **34**: 23-37.

Teodor ED, Ungureanu O, Gatea F and Radu GL (2020). The potential of flavonoids and tannins from medicinal plants as anticancer agents. *Anticancer Agents Med. Chem.*, **20**(18): 2216-2227.

Thomford NE, Senthebane DA, Rowe A, Munro D, Seele P, Maroyi A and Dzobo K (2018). Natural products for drug discovery in the 21st century: Innovations for novel drug discovery. *Int. J. Mol. Sci.,* **19**: 1578.

Thorngren DP, Fortney JJ, Murray-Clay RA and Lopez ED (2016). The mass-metallicity relation for giant planets. *Astrophys. J.,* **831**(1): 64.

Uzzaman M, Hasan MK, Mahmud S, Fatema K and Matin MM (2021). Structure-based design of new diclofenac: Physicochemical, spectral, molecular docking,

dynamics simulation and ADMET studies. *Inform. Med. Unlocked.*, **25**(2021): 100677.

Wang FX, Li HY, Li YQ and Kong LD (2020). Can medicinal plants and bioactive compounds combat lipid peroxidation product 4-HNE-induced deleterious effects? *Biomol.,* **10**(1): 146.

Wass MN, Kelley LA and Sternberg MJ (2010). 3DLigandSite: Predicting ligand-binding sites using similar structures. *Nucleic. Acids Res.,* **38**(1): 469-473.

Yang J, Roy A and Zhang Y (2013). Protein–ligand binding site recognition using complementary binding-specific substructure comparison and sequence profile alignment. *Bioinform.,* **29**(1): 2588-2595.

Ye M, Dewi L, Liao YC, Nicholls A, Huang CY and Kuo CH (2023). DNA oxidation after exercise: A systematic review and meta-analysis. *Front. physiol.*, **14**: 1275867.

Zhang Z, Li Y, Lin B, Schroeder M and Huang B (2011). Identification of cavities on protein surface using multiple computational approaches for drug binding site prediction. *Bioinform.,* **27**(15): 2083-2088.